buildings

MDPI

Article

Passive Dissipation of Canopy Urban Heat Through Double Skin Façades

Chih-Hong Huang [1], Ching-Hsun Wang [2,*] and Yu-Ping Tsaur [1]

[1] Department of Architecture, National Taipei University of Technology, Taipei City 10608, Taiwan; huangch@mail.ntut.edu.tw (C.-H.H.); peterpeter0528@gmail.com (Y.-P.T.)
[2] College of Design, National Taipei University of Technology, Taipei City 10608, Taiwan
* Correspondence: eric.wang.xun@gmail.com

Abstract: In the face of global warming, mitigating the urban heat island effect has become an important concern worldwide. This study applies the principle of buoyancy ventilation formed by sunlight in double skin façades (DSFs) to improve the thermal environment outside buildings by discharging heat through temperature and pressure differences. The study subject is a 15 × 30 × 40 m residential concrete building situated in a subtropical climate. The lower opening of the DSF faces the outdoor environment; heat is absorbed through this opening from the ground environment and then evacuated up to above the urban canopy layer heat island in order to cool pedestrian environments on the ground. We used numerical simulation to analyze the cooling potential of this DSF in summer daytime conditions. The results show that the DSF can successfully transport heat energy and discharge it above the urban canopy layer. Significant cooling effects were observed in both the horizontal and vertical spaces on the leeward side of the building DSF through the passage of surface heat, thereby reducing the load of indoor air conditioning.

Keywords: urban canopy layer heat island; surface urban heat island; double skin façades; passive design

check for updates

Received: 14 December 2024
Revised: 24 January 2025
Accepted: 27 January 2025
Published: 29 January 2025

Citation: Huang, C.-H.; Wang, C.-H.; Tsaur, Y.-P. Passive Dissipation of Canopy Urban Heat Through Double Skin Façades. *Buildings* **2025**, *15*, 430. https://doi.org/10.3390/buildings15030430

Copyright: © 2025 by the authors. Licensee MDPI, Basel, Switzerland. This article is an open access article distributed under the terms and conditions of the Creative Commons Attribution (CC BY) license (https://creativecommons.org/licenses/by/4.0/).

1. Introduction

The urban heat island (UHI) effect occurs when urban temperatures are higher than those in neighboring rural or suburban areas [1]. The intensity of the effect is quantified through the temperature difference between urban and rural areas [2]. Due to rapid urbanization, dense infrastructure, and global warming, many cities are suffering from UHI-related environmental and social challenges [3]. Oke [4] divided UHI types into boundary heat (UHI_{UBL}), canopy heat (UHI_{UCL}), surface heat (UHI_{Surf}), and underground heat (UHI_{Sub}). UCL originates in a three-dimensional urban canyon environment composed of buildings, floors, and roofs [5]. The impacts of the urban built environment and energy-saving building renovations on microclimates have attracted increasing attention [6], with the strongest focus on UCL [7]. The building mass and the configuration of building materials in urban areas have a significant impact on the thermal environment [8]. Urban built environments absorb, diffuse, and reflect incident solar radiation more than natural land [9]. Thus, UHIs continue to intensify as natural landscapes shift to built landscapes [10].

Roughly one-third of global energy consumption can be attributed to commercial and residential buildings; this statistic is likely to increase to almost half by the end of 2025 [11]. Global warming and UHIs have caused urban temperatures to rise, significantly increasing the energy demand for cooling [12]. At the same time, decreasing global energy

resources and increasing energy costs have prompted the construction industry to reduce energy expenditures [13]. Effectively reducing building energy consumption has become key to energy conservation [14]. Thus, reducing heating and cooling loads to improve building energy performance and maintain occupants' thermal comfort has become a major challenge [15].

In the search for solutions to reducing energy demand [16], building façades have been found to exert a significant impact on building energy demand and occupants' thermal comfort [17]. In particular, double skin façades (DSFs) are gaining attention as an important passive design [18]. DSFs consist of two parallel transparent layers, which can be single or multiple glass units, that form an air cavity [19]. The bottom and top of the air cavity are vents that can be opened and closed. When the vents are open, they contribute to natural ventilation [20]. Air cavities have the potential to enhance building performance [21] by creating pressure differences driven by thermal buoyancy and by allowing spaces for wind to blow [22]. The buoyancy force caused by temperature differences is called the chimney effect [23]. DSFs are increasingly popular in practice because they are visually appealing as well as quick and easy to build. However, research on their climate-related performance remains limited [24]. Sharston and Singh [25] showed that the thermal insulation performance of the building envelope of passive components is critical to energy consumption. Building technology that provides natural ventilation can help to achieve sustainable strategies to meet green goals for 2030 and 2050 [26]. Although DSFs have many applications, there are gaps in research regarding system optimization, control strategies, and optimization dynamics [27]. Darkwa et al. [28] studied the flow field of a DSF office building and found that in summer, the top of the DSF was 4.6 °C above the ambient temperature, indicating that increasing the ventilation rate of the DSF would improve the energy efficiency of the building.

Buildings have a close and complex relationship with their external environments [29]. At present, most DSF-related research has focused on building energy and indoor temperatures; few studies have focused on the outdoor thermal environment of buildings. The current paper thus qualitatively evaluates the cooling potential of a DSF on the surface temperature of outdoor urban environments. The proposed device passively transports heat from the ground surface and the building itself to the top of the urban canopy, and high-speed airflow in the upper floors is used to achieve cooling in the canopy. In view of the hot and humid subtropical summer urban climate, this study evaluates the cooling potential of DSFs at near-surface temperature and pedestrian height in an urban thermal environment under a subtropical climate, links the DSF system with urban thermal environment issues, and proposes strategies and contributions to the field.

2. Materials and Methods

2.1. Research Background

Taipei is the center of Taiwan's political and economic development. It has a longitude of 121.56 degrees, a latitude of 25.09 degrees, and a population of approximately 2.5 million. The land is located in the Keelung River and Tamsui River basins. It is affected by the surrounding mountains, with year-round easterly winds and high humidity. The research context is a 15 × 30 × 40 m building situated in this subtropical climate. The building is assumed to be made of concrete, with the surrounding ground covered by asphalt, which is close to the real environment, and some paving surfaces are concrete. In order to achieve the high-density residential environment of the study area, the buildings in the simulation were made of concrete and the surrounding ground was asphalt road, which is consistent with the actual environment. We refer to this combination as the "original plan" and simulate the thermal performance and flow field changes of materials and

building heat storage bodies under solar radiation from 8 a.m. to 2 p.m. The source of summer temperature, wind speed, and solar radiation data is the Taiwan Central Weather Administration (https://codis.cwa.gov.tw/) [30] (Accessed on 1 August 2023). At this time, the building DSF absorbs a large amount of heat energy and has the most vigorous natural ventilation effect. As the temperature drops at night, people's thermal comfort improves.

The DSF shows that there is a direct causal relationship between the canopy heat island and the intensity of solar radiation; that is, the stronger the canopy heat island, the stronger the chimney effect. There are rarely phenomena of urban high temperatures in the study area during spring, autumn, and winter. DSF ventilation is not strong, or the DSF ventilation pipe can be closed.

The process framework of this research is shown in Figure 1.

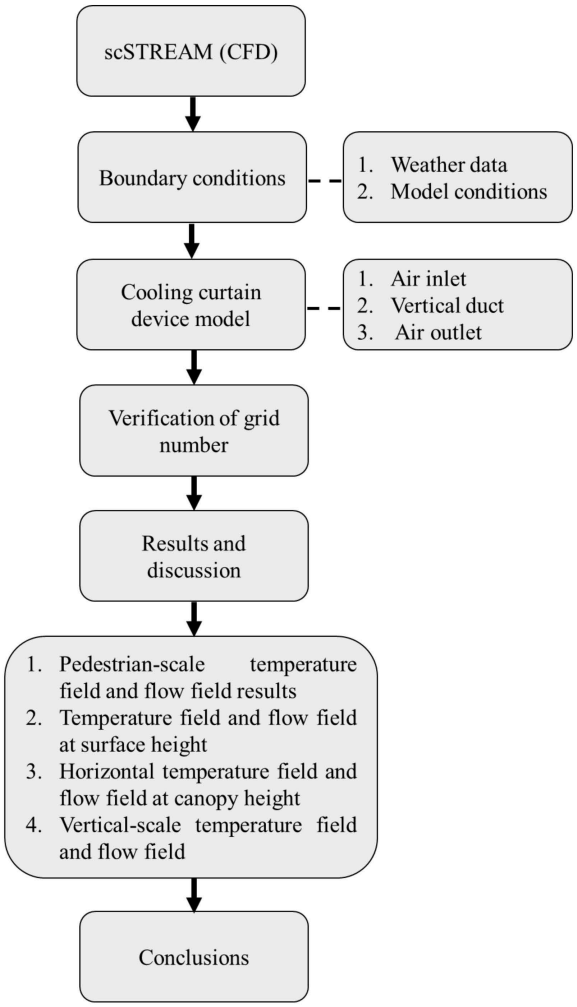

Figure 1. Flowchart of research framework.

2.2. Boundary Conditions

CFD technology has been widely adopted to study the thermal performance of ventilated DSFs [31]. The numerical analysis in this study was conducted with scSTREAM, software that has a high degree of computational efficiency and is highly integrated from pre- to post-processing stages. The applications of this software range from electronic parts to the multi-scale flow field analysis of urban wind fields.

It is important to set the temperature and airflow of each surface in order to perform the analysis, and the balance between the incoming airflow and the air outlet is also important [32]. The parameters used in scSTREAM in this study are shown in Table 1.

These include an ambient temperature of 34 °C, gradient wind speed of 1.5 m/s, and solar radiation of 853.83 W/m^2. The solar radiation, wind speed, and ambient temperature values selected in this study are based on the local average midday temperature and sunshine in August. The boundary conditions were set to represent the state when the canopy heat island is the most severe during the local midsummer in August.

Table 1. Boundary conditions for numerical simulation.

Settings	Boundary Condition	Parameter
Inlet	Low power boundary	V_{10} = 1.5 m/s, 34 °C
Outlet	Static pressure boundary	-
Left, right, up	Free slip *	-
Down	No slip **	-
Solar	Solar radiation	853.83 W/m^2
Temperature	Ambient temperature	34 °C

* The free sliding boundary condition stipulates that the fluid can slide freely on the boundary surface, but not on the boundary. ** A no-slip boundary condition states that a fluid layer in contact with a solid boundary must have the same velocity as that boundary.

The simulation is performed using transient analysis to evaluate the hourly changes in the flow field over time. The turbulence model uses a linear low-Reynolds number (AKN). This model is aimed at improving the prediction accuracy in the near-wall area, which is most important for studying phenomena in turbulence. The size of the calculation domain is based on the F guideline. Franke et al. [33] suggested that the top (upwind) and lateral boundaries should be at least 5H away from the model (H refers to the highest height of the building), and the exit (downwind) should be at least 15H away to allow for the development of wakes (see Figure 2). A simulation was conducted based on the original plan, which was composed of a single building volume and asphalt pavement. Another simulation was then performed to explore the cooling improvement effect at different scales before and after the installation of the proposed DSF. Based on our results, we put forward suggestions for buildings in subtropical hot and humid climate settings.

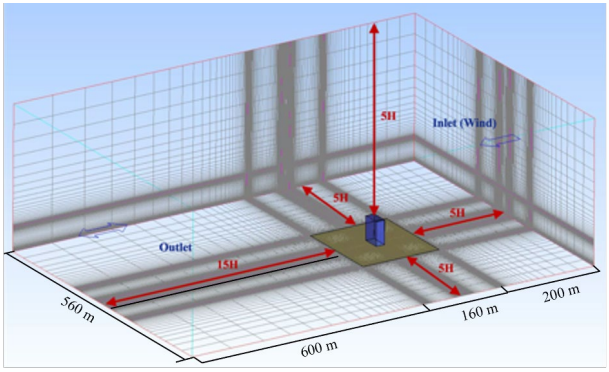

Figure 2. Original solution model and computational domain boundaries.

2.3. Proposed Model

The purpose of this study was to seek a means of improving the microclimate conditions of air temperature and low wind speed within the urban canopy heat island through the design of a DSF. Climates with higher wind speeds or lower solar radiation have less severe canopy heat islands. The proposed device comprises (1) an air inlet, (2) a vertical duct, and (3) an air outlet (Figure 3). The air inlet is used to connect to the urban ground surface. It is located one floor (4 m) above the ground. This allows for future installations, and the absorption of ground temperature is ensured through changes in pipe diameter

(1.2 m to 0.6 m). The vertical pipe is 36 m high and 0.6 m wide. In order to avoid turbulence blocking the airflow during the rising process, the 30 m wide pipe is divided into five units. The height where the building connects to the urban canopy is set with reference to the work of Ding et al. [34]. The DSF outlet is set at a height of 8 m (two floors above the roof) to obtain sufficient pressure difference distribution. This not only improves ventilation effects but also solves the problem of overheating in the exterior wall of the DSF [28]. The DSF is made of glass (see Figure 4). Detailed material parameters are shown in Table 2.

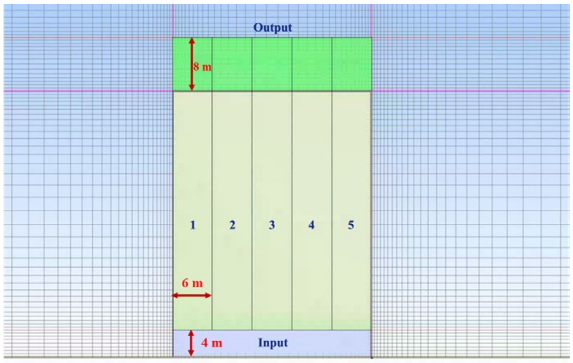

Figure 3. The dimensions of the DSF.

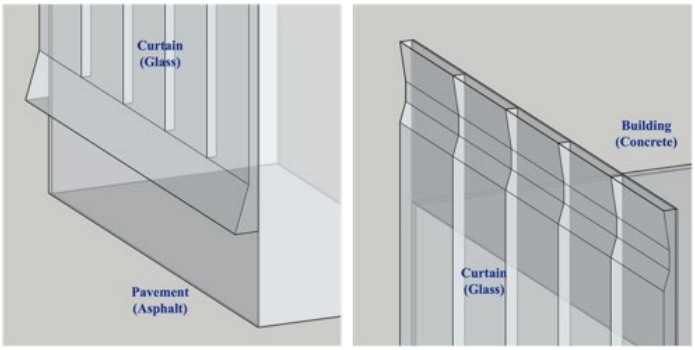

Figure 4. Lower and upper openings of proposed DSF.

Table 2. Building material parameters used in the model.

Settings	Material	Density (kg/m^3)	Specific Heat (J/kg·K)	Thermal Conductivity (W/m·K)	Reflectance	Absorbance	Transmittance
Ground	Asphalt	2120	920	0.74	0.2	0.8	-
Building	Concrete	2400	900	1.2	0.5	0.5	-
Curtain wall	Glass	2190	740	1.38	0.05	0.05	0.9

2.4. Verification of Grid Number

As ventilation is the buoyancy driver in the cavity, it is important to have a fine-enough mesh to solve for the thermal boundary layer [35]. The main purpose of validation is to confirm the accuracy of the computational model as a solution [36]. In transient analysis, a larger time step reduces the simulation accuracy and calculation stability. Thus, the time step must be small enough to ensure the accuracy and stability of the simulation. The Courant number is used in the scSTREAM simulation software to ensure the quality of the modeling process data (Equation (1)). In addition, the physical quantities of numerical simulation were used to verify the grid accuracy (Figure 5), and the temperature sampling on the leeward side of the model was used to calculate the error. The overall accuracy fell within the range of approximately ±1%. It is sufficient to set the error range of the grid to

±1%. A finer grid leads to a significant increase in the amount of calculation, which may lead to failure to converge.

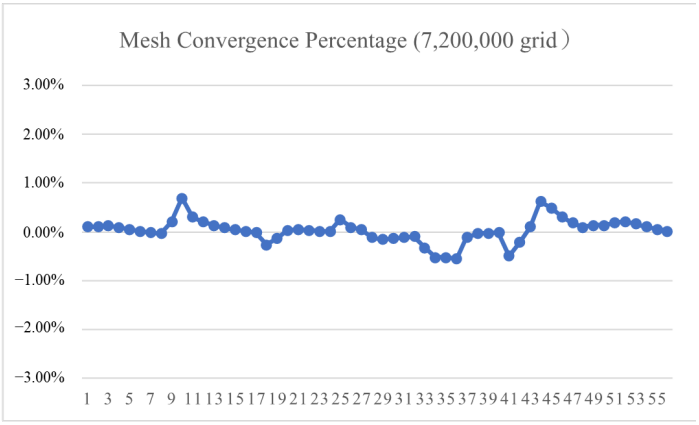

Figure 5. Grid number verification.

The empirical data related to canopy heat island measurements are roughly consistent with the phenomena in this study [37].

$$C = \frac{\Delta t \times u}{\Delta L} \leq 1 \quad (1)$$

where

C: Courant number;
Δt: time step;
u: interpolated value of velocity at center of element;
ΔL: element width.

3. Results and Discussion

We discuss the performance of the proposed DSF solution under the following three categories. (1) We analyzed the temperature field and airflow field changes at pedestrian height to determine the effects of the proposed device on human thermal comfort and health. (2) We analyzed the temperature field and flow field in the horizontal direction at pedestrian height on the ground surface and at the landscape height to evaluate the surface cooling potential of the proposed device. (3) The vertical-scale temperature field and flow field around the building were used to evaluate the vertical transport of surface heat by the double-layer curtain exterior wall, the heat transfer performance of the pipes, and the calorimetric heat emission to the canopy.

The DSF device proposed in this study was simulated with CFD. The results show that it can transfer surface heat energy to the urban canopy, achieving the effect of reducing the temperature near the surface scale and at pedestrian height around the building. It is also expected that surface heat will be carried away by wind farms above high-rise buildings. However, this study has some limitations. Since it involves the scale of urban canopies and is related to the massing design of the entire building, it is difficult to conduct experiments through the actual installation of DSFs.

3.1. Pedestrian-Scale Temperature Field and Flow Field

Figure 6 shows the horizontal temperature and airflow results at a pedestrian height of 1.5 m after 6 h of transient analysis. In the original plan on the left, it can be seen that the vortices caused by the airflow passing through the sides of the building accumulate heat on the leeward side. The accumulated heat in the leeward and shadowed areas of the

building is effectively extracted by the vertical air ducts and cooled. Under the proposed plan on the right, the heat that originally existed in the building is sucked in through the pipe inlet close to the ground, which greatly improves the overheating problem on the leeward side of the building, alleviates the vortex that originally existed in the leeward side of the building, and effectively improves thermal comfort for pedestrians.

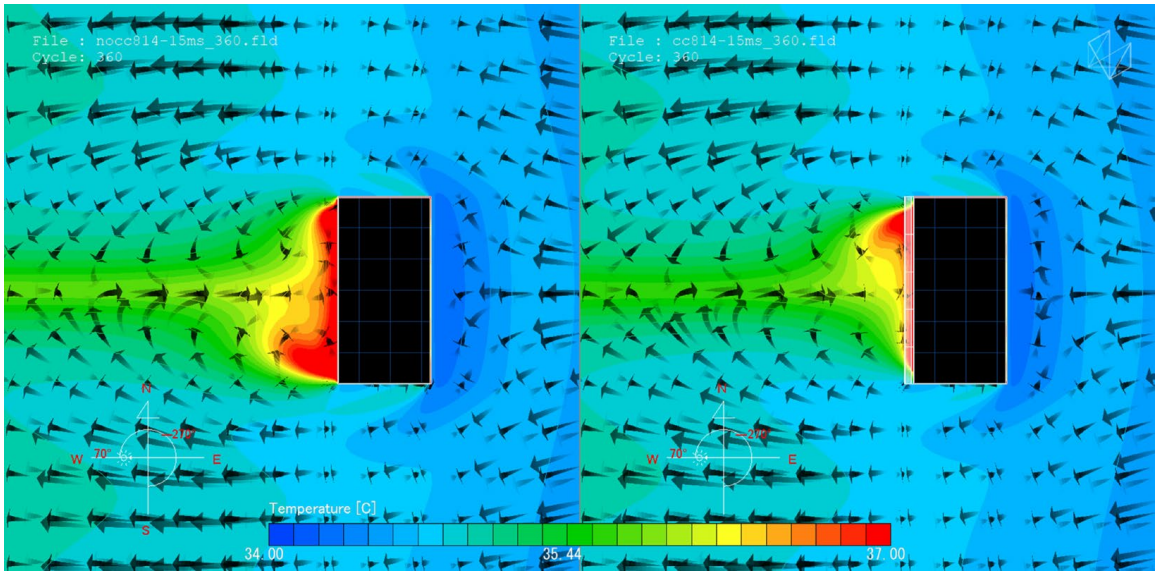

Figure 6. Temperature and flow field distribution at a pedestrian height of 1.5 m: (**left**) original plan; (**right**) proposed plan.

Figure 7 shows the point conditions on the leeward side of the building, which were used to quantify the parameters of each point and observe the temperature difference results at pedestrian height. At the air inlet 1.5 m from the building level, there is a maximum cooling of 2.15 °C (Table 3). The temperature gradient of the canopy heat island at pedestrian height is obviously channeled and cooled. At the same time, a drop in temperature was observed under the DSF 30 m from the building. In the middle area on the leeward side, a temperature increase of 0.02 °C to 0.23 °C was observed compared to the original plan, indicating that the heat inhalation under the proposed DSF concentrates the heat dissipated from the ground.

Table 3. Temperature differences between proposed and original plans at varying pedestrian heights (°C).

(m) X Y	0.5	1.5	5	10	15	20	25	30
−3	−0.03	−0.05	−0.13	−0.15	−0.12	−0.09	−0.06	−0.04
3	−0.91	−2.15	−2.11	−1.09	−0.58	−0.35	−0.22	−0.15
9	−0.35	−0.54	−0.72	−0.91	−0.63	−0.40	−0.26	−0.18
15	−0.32	−0.34	−0.25	−0.25	−0.24	−0.21	−0.18	−0.17
21	−0.21	−0.15	0.21	0.23	0.03	−0.04	−0.07	−0.08
27	−0.35	−0.30	0.15	0.02	−0.02	−0.03	−0.04	−0.03
33	0.01	−0.01	−0.06	−0.05	−0.03	−0.01	0.00	0.00

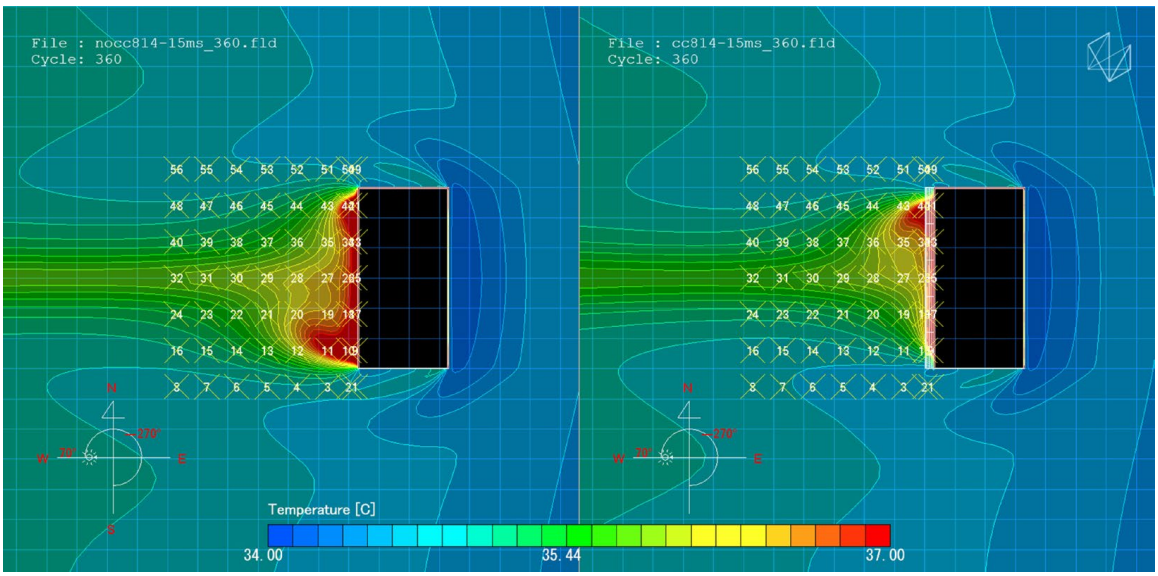

Figure 7. Temperature difference at horizontal points at a pedestrian height of 1.5 m: (**left**) original plan; (**right**) proposed plan.

3.2. Temperature Field and Flow Field at Surface Height

Figure 8 shows the temperature and flow field results at a distance of 0.5 m from the ground. Compared with pedestrian height, this height analysis evaluates the heating of the ground surface and the adsorption capacity of pipe devices after the building materials absorb heat. The results in Figure 9 show that the proposed device has a cooling effect of up to 3.12 °C on the surface temperature (Table 4). At pedestrian height, a similar decrease in surface temperature is observed within a range of 30 m from the building. This shows the potential of the device in cooling the ground surface. It is suggested that a comprehensive study be conducted in conjunction with urban-related land planning elements such as greening, water bodies, and cooling materials. The proposed solution is expected to effectively improve the urban thermal environment and indoor heat load and create a more comfortable outdoor walking environment.

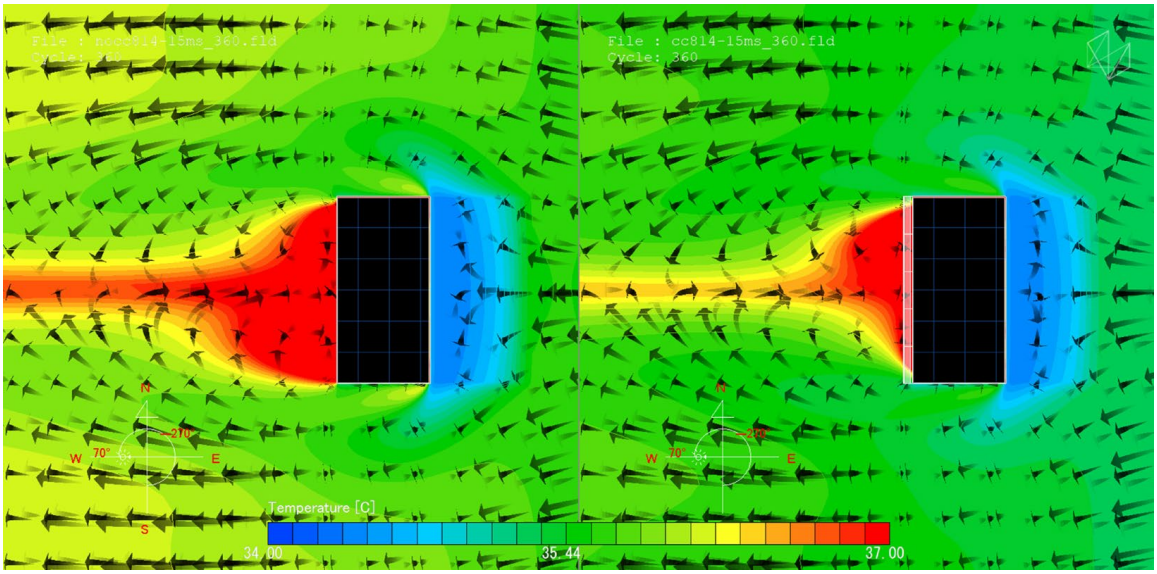

Figure 8. Temperature and flow field distribution at a surface height of 0.5 m: (**left**) original plan; (**right**) proposed plan.

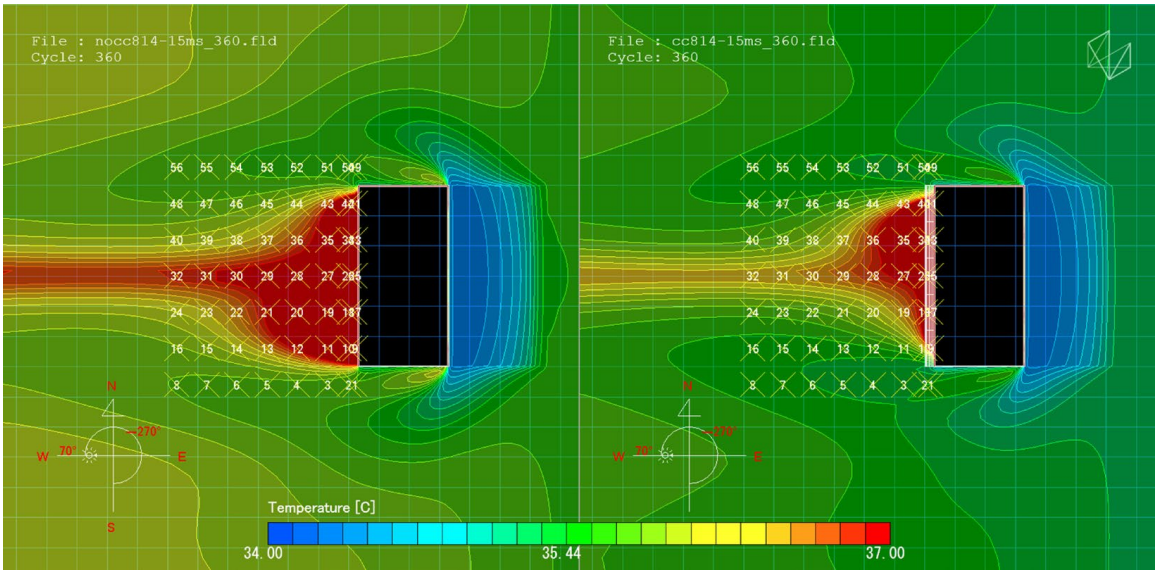

Figure 9. Temperature difference at a horizontal point at a height of 0.5 m above the ground: (**left**) original plan; (**right**) proposed plan.

Table 4. Differences in surface temperature between proposed and original plans(°C).

(m) X / Y	0.5	1.5	5	10	15	20	25	30
−3	−0.26	−0.28	−0.35	−0.38	−0.36	−0.34	−0.32	−0.30
3	−1.29	−3.12	−2.79	−1.53	−0.95	−0.66	−0.50	−0.41
9	−0.72	−1.03	−1.12	−1.52	−1.08	−0.75	−0.56	−0.45
15	−1.08	−0.72	−0.65	−0.64	−0.60	−0.55	−0.51	−0.48
21	−1.04	−0.69	0.03	0.13	−0.14	−0.25	−0.29	−0.31
27	−1.65	−1.59	−0.19	−0.20	−0.21	−0.24	−0.25	−0.26
33	−0.14	−0.15	−0.20	−0.22	−0.22	−0.22	−0.23	−0.24

DSF building façades have become a solution adopted by modern high-rise building construction technology without incurring too much additional cost. However, the comfort of the outdoors in summer promotes urban culture and social exchange processes in public spaces, which has a high value.

3.3. Horizontal Temperature Field and Flow Field at Canopy Height

Figure 10 shows the temperature and flow field results of the proposed and original plans under 6 h transient analysis at a height of 48 m. This height is the position of the air outlet. After solar radiation reaches the surface, the heat absorbed by the ground and the building shell is transported through the DSF duct to an outlet located two floors above the roof height for discharge.

The temperature and wind field at an altitude of 48 m clearly show that the hot air near the ground is being channeled to high altitudes. The high-altitude heat flow also produces displacement and is gradually carried away from the building base.

The results in Figure 11 show that the maximum temperature difference between the pipeline outlet and the original plan is 3.2 °C (Table 5). The heat discharged from the pipe outlet is carried away from the ground by the high-speed airflow at canopy height. This shows that surface heat is effectively piped to the upper canopy. The trend of heat

movement in the canopy over longer periods of time and the thermal behavior at night need to be further explored to fully understand the distribution of heat in different time periods.

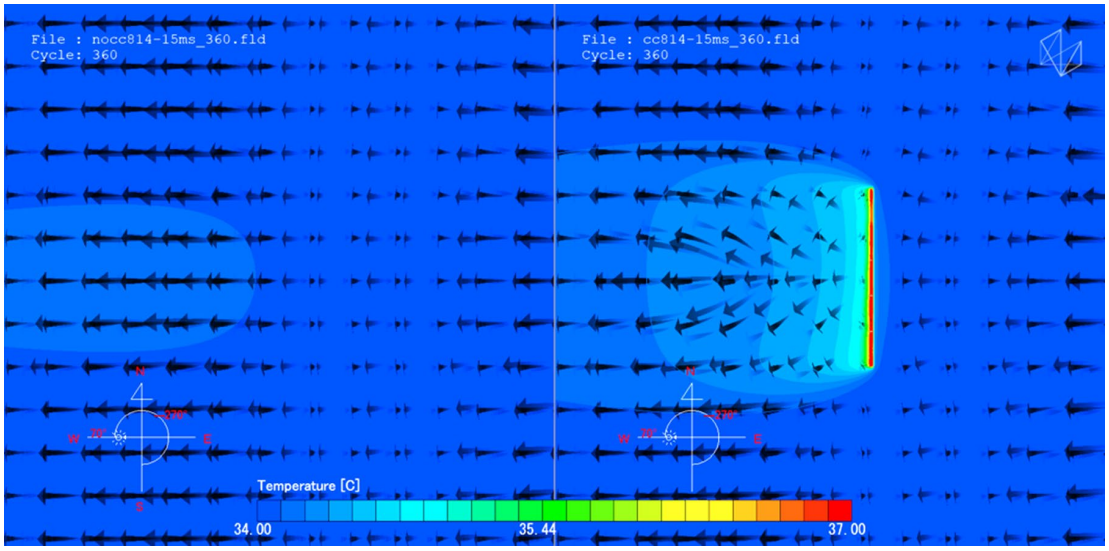

Figure 10. Temperature and flow field distribution at the canopy exit height of 48 m: (**left**) original plan; (**right**) proposed plan.

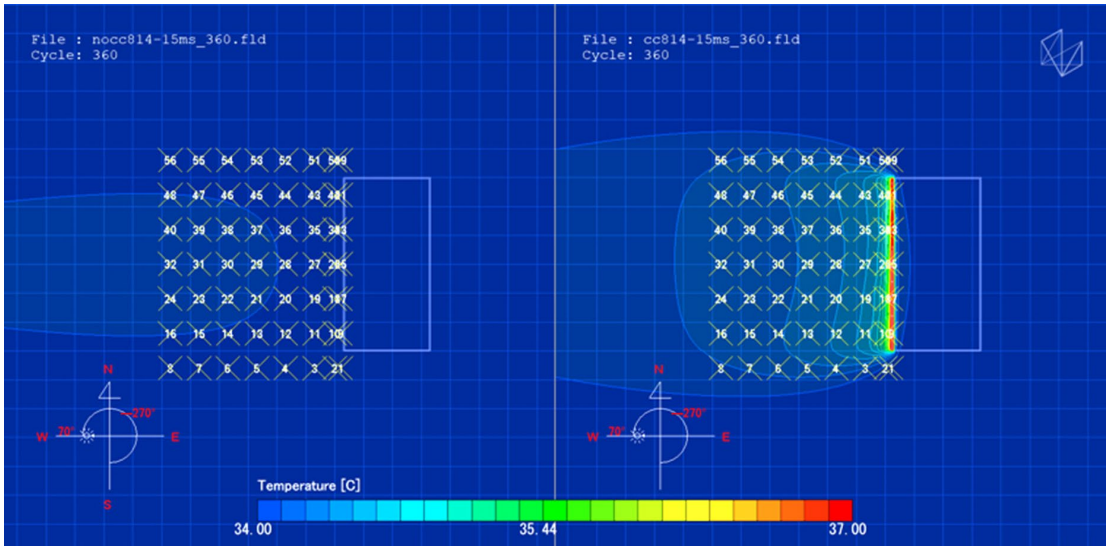

Figure 11. Temperature difference at horizontal points at canopy exit height of 48 m: (**left**) original plan; (**right**) proposed plan.

Table 5. Canopy temperature differences between proposed and original plans (°C).

(m) X / Y	0.5	1.5	5	10	15	20	25	30
−3	0.06	0.09	0.23	0.31	0.29	0.25	0.21	0.17
3	3.14	1.27	0.62	0.44	0.32	0.24	0.19	0.15
9	3.22	1.15	0.56	0.37	0.26	0.18	0.13	0.10
15	3.01	1.01	0.52	0.35	0.23	0.16	0.11	0.09
21	2.72	0.92	0.52	0.36	0.25	0.18	0.13	0.10
27	2.53	0.95	0.56	0.42	0.31	0.24	0.19	0.15
33	0.05	0.08	0.21	0.30	0.29	0.25	0.21	0.18

3.4. Vertical Temperature Field and Flow Field

Through vertical temperature field and flow field analysis, we can understand the movement and distribution of heat in the urban canopy. Under the original plan (Figure 12), solar radiation heats the ground surface, producing significant heat emissions in the building shell and ground surface. In urban environments, the increase in surface roughness caused by densely distributed building volumes and pavements causes the wind speed to decrease significantly closer to the surface. At the same time, the downdraft that exists around the building sinks heat to the leeward side of the building.

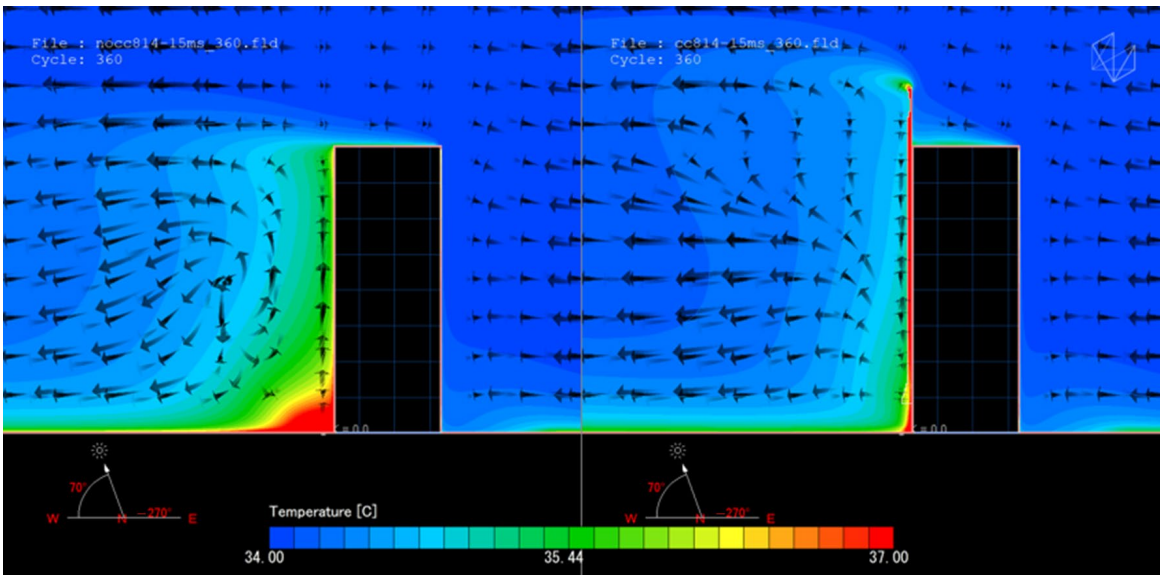

Figure 12. Temperature and flow field distribution in vertical section of urban canopy: (**left**) original plan; (**right**) proposed plan.

DSFs greatly improve the original accumulation of high temperature on the ground. The heat existing on the ground and around the building is concentrated in the curtain ducts and transported to the top of the canopy for discharge.

In the proposed plan, the air inlet openings at the bottom facing the ground draw the heat existing on the ground and around the building away from the ground. The highest temperature drop of 2.83 °C was observed at 1.5 m from the building (Figure 13) (Table 6). Moreover, the temperature is reduced in the building height range of 0 to 40 m, thereby improving human thermal comfort. A temperature inversion was observed at a height of 45 m at the air outlet, indicating that the heat was transferred through the pipe to the outlet at the top and discharged.

Since there is a higher wind speed area above the building height, when the surface heat energy is transferred above the urban canopy through the cooling curtain wall device, it is expected that the heat energy will be carried away by the high wind speed.

Compared to other strategies, although building green walls can reduce temperatures in the study area as well, they do, however, increase urban humidity and thermal enthalpy. Moreover, the humidity and heat enthalpy accumulate in the already severe canopy heat island area. In a marine climate with high temperature and high humidity, the human body suffers from thermal discomfort.

Cool roofs cannot reduce temperatures at pedestrian height. Sunshade devices are not suitable for use in high-density residential areas and are restricted by relevant regulations.

For the subtropical summer urban climate with a hot and humid environment, the DSF shows its significant effect of driving heat energy up around the building site. And the hotter the weather, the stronger the updrafts are, achieving a greater heat dissipation effect.

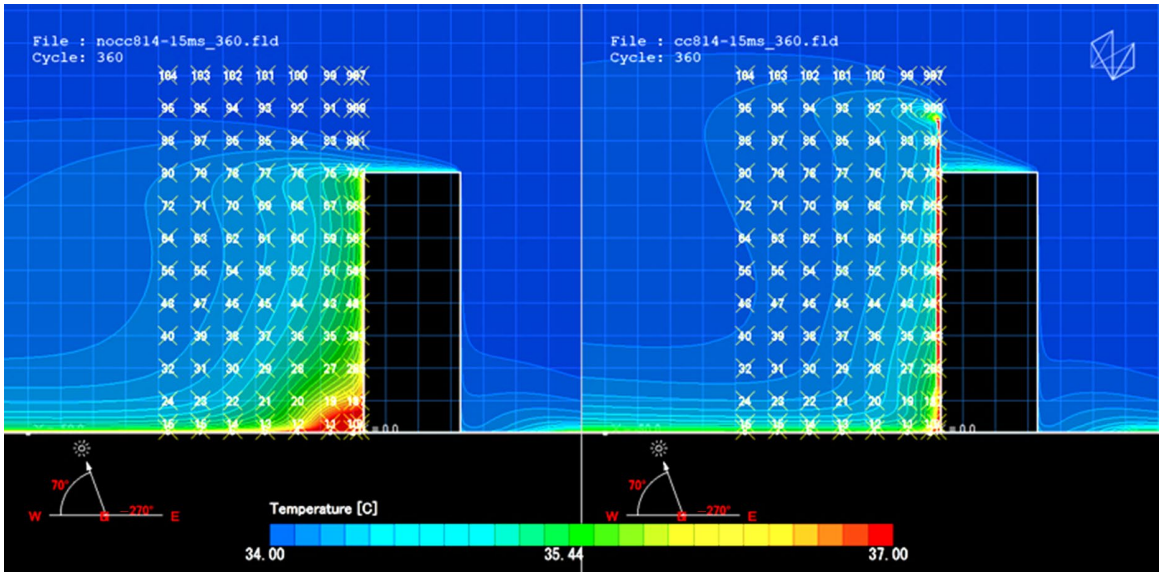

Figure 13. Point distribution of urban canopy: (**left**) original plan; (**right**) proposed plan.

Table 6. Vertical point temperature differences between proposed and original plans (X0.5 is the DSF position) (°C).

(m) X / Z	0.5	1.5	5	10	15	20	25	30
0.5	−1.06	−2.83	−2.48	−1.27	−0.72	−0.45	−0.30	−0.22
1.5	−0.91	−2.15	−2.11	−1.09	−0.58	−0.35	−0.22	−0.15
5	−0.37	−0.97	−1.22	−0.91	−0.56	−0.35	−0.23	−0.17
10	0.55	−0.63	−0.65	−0.56	−0.42	−0.31	−0.23	−0.18
15	1.03	−0.51	−0.46	−0.39	−0.32	−0.26	−0.21	−0.18
20	1.41	−0.45	−0.38	−0.31	−0.26	−0.22	−0.19	−0.16
25	1.73	−0.43	−0.35	−0.28	−0.24	−0.20	−0.17	−0.15
30	2.00	−0.43	−0.33	−0.27	−0.23	−0.19	−0.16	−0.14
35	2.21	−0.50	−0.37	−0.30	−0.25	−0.21	−0.17	−0.14
40	2.76	−0.38	−0.34	−0.29	−0.23	−0.18	−0.14	−0.10
45	0.81	0.59	0.41	0.25	0.14	0.09	0.06	0.04
48	3.73	1.09	0.60	0.43	0.31	0.24	0.18	0.14
53	0.07	0.11	0.25	0.32	0.31	0.27	0.23	0.20

4. Conclusions

This study explores the heat absorbed and emitted by a building and the ground surface due to solar radiation and compares this heat to that of a building with an exterior DSF under summer conditions. The proposed DSF uses its own natural heat convection to form a passive and continuous heat transfer mechanism to raise the surface heat to the height of the urban canopy and then discharge it. The heat is dissipated through the smooth urban wind field above the top of the building, that is, above the canopy heat island. The results show that the proposed DSF has a good cooling effect on the urban horizontal and vertical scales, effectively alleviating the problem of high-temperature accumulation on the urban microclimate scale. Our findings lay the foundation for further research on reducing indoor air conditioning energy consumption and energy usage. We provide new insights into the impact of DSFs on the outdoor environment of buildings and their benefits to

urban canopy heat islands. In the following, we outline some important conclusions and planning suggestions for subtropical urban and architectural design.

4.1. Cooling Potential of DSFs in Near-Surface Layer

We conducted cross-sectional discussions on the flow field at the surface height near the ground layer, the height where pedestrians have the most intensive activities, and the DSF exit height of the urban canopy. We showed that the proposed device has great cooling potential for the canopy heat island and brings a comfortable ambient temperature to the leeward part of the building compared with the original plan, with a maximum temperature difference of 3.12 °C.

As urban temperatures continue to rise year by year, if the installation of duct cooling DSFs can be taken into consideration when designing buildings in urban areas, it is expected that the near-surface temperature can be gradually improved.

4.2. Vertical Heat Transport and Transfer by DSF

The maximum temperature difference of 2.83 °C was observed at the near-surface level, indicating that the air inlet opening at the bottom of the pipeline effectively sucks the high surface temperature into the interior of the pipeline. This heat is passed all the way to the top of the urban canopy through vertical pipes for drainage. The internal division of the pipe helps to stabilize the turbulence that occurs when the airflow is upward, achieving continuous passive cooling. This effect can be further improved by adding materials and equipment in the pipes for increased heat transfer and considering whether installing DSFs on the four façades of the building can better improve the near-surface air temperature and thermal comfort at pedestrian height.

4.3. Application of DSFs in Site Planning

The current paper focuses on heat dissipation by a DSF for a single building volume and evaluates the improvement effect of this single device on the urban canopy heat island. Further research on building cooling should include coupling analysis combining different floor plans, wind tunnel test verification of scale models, and quantitative analysis of the benefits of DSFs in improving urban thermal environments. The installation direction and location of the device should be considered and analyzed in more detail, including contexts such as buildings above a specific height and wind corridor flow areas. Elucidation of these phenomena would ensure that the heat discharged in the canopy does not flow back to the lower part of the urban canopy.

The results of this study can be used as a reference for government departments and architects. When there is a city-wide integrated wind field masterplan analysis, it can be applied to the design specifications of future new building codes.

Further research should consider the existing massing of surrounding buildings and evaluate how the design of new buildings fits in with the surrounding building clusters and urban design.

4.4. Building Design Guidelines or Policies for Urban Planning

A city-wide integrated wind field analysis is necessary. After analyzing the midsummer wind field and coordinating with the community's outdoor surface hot spot diagnosis, the pedestrian hot zone is strengthened with DSF heat diversion. Developing an effective canopy heat island (vertical) ventilation program is completely conceivable in future smart city planning.

In addition to providing design considerations for new buildings, this can also provide suggestions for the repair or renovation of existing building façades and establish guidelines for improving the urban thermal environment.

5. Future Research Needs and Opportunities

As the weather becomes more and more diverse, future research may not only consider the average weather condition parameters, but also continue to explore the effectiveness of DSFs under different weather conditions (summer sunny days, summer rainy days, etc.) and develop DSFs that are more suitable for various meteorological conditions to mitigate the negative impact of extreme high temperatures on the public.

In addition, research should be conducted on the thermal environmental effects of DSFs in multiple buildings, building clusters, or urban designs.

With global warming, cities around the world are facing the issue of increasing temperatures year by year. Therefore, it is necessary to combine architectural technology and urban planning expertise as soon as possible to jointly propose effective improvement strategies. The results of this study can be provided to government urban planning departments and construction professionals as a reference for building laws and architectural designs.

Author Contributions: All authors contributed to the research content. Conceptualization, C.-H.H.; methodology, C.-H.H.; project administration, C.-H.W.; software, Y.-P.T.; supervision, Y.-P.T.; validation, Y.-P.T.; writing—original draft, C.-H.W.; writing—review and editing, C.-H.W. All authors have read and agreed to the published version of the manuscript.

Funding: This research was funded by the [Research Center of Energy Conservation for New Generation of Residential, Commercial, and Industrial Sectors] and [MOE Teaching Practice Research Program (MOE-113-TPRSR-0025-001Y1)] and [National Science and Technology Council (NSTC) Project No. 110-2221-E-027-018-MY2]. The APC was funded by the [Research Center of Energy Conservation for New Generation of Residential, Commercial, and Industrial Sectors] and [MOE Teaching Practice Research Program (MOE-113-TPRSR-0025-001Y1)].

Data Availability Statement: The data resulting from this study are included in the article, and the authors can provide further data upon reasonable request.

Acknowledgments: The funders and National Taipei University of Technology are gratefully acknowledged.

Conflicts of Interest: The authors declare that there are no conflicts of interest between the research presented in this paper and its authors and publishers.

References

1. Kumar, A.; Mukherjee, M.; Goswami, A. Inter-Seasonal Characterization and Correlation of Surface Urban Heat Island (SUHI) and Canopy Urban Heat Island (CUHI) in the Urbanized Environment of Delhi. *Remote Sens. Appl. Soc. Environ.* **2023**, *30*, 100970. [CrossRef]
2. Kamal, A.; Mahfouz, A.; Sezer, N.; Hassan, I.G.; Wang, L.L.; Rahman, M.A. Investigation of Urban Heat Island and Climate Change and Their Combined Impact on Building Cooling Demand in the Hot and Humid Climate of Qatar. *Urban Clim.* **2023**, *52*, 101704. [CrossRef]
3. Mughal, M.O.; Li, X.X.; Norford, L.K. Urban Heat Island Mitigation in Singapore: Evaluation Using WRF/Multilayer Urban Canopy Model and Local Climate Zones. *Urban Clim.* **2020**, *34*, 100714. [CrossRef]
4. Oke, T.R. The Heat Island of the Urban Boundary Layer: Characteristics, Causes and Effects. In *Wind Climate in Cities*; Cermak, J.E., Davenport, A.G., Plate, E.J., Viegas, D.X., Eds.; Springer: Dordrecht, The Netherlands, 1995; pp. 81–107.
5. Oke, T.R. *Boundary Layer Climates*, 2nd ed.; Routledge: London, UK, 2002.
6. Chen, C.; Wang, J.; Zhang, H.; Xu, X.; Hinkle, L.E.; Chao, X.; Shi, Q. Dual Impacts of Solar-Reflective Façades in High-Density Urban Areas on Building Energy Use and Outdoor Thermal Environments. *Energy Build.* **2024**, *324*, 114926. [CrossRef]
7. Oke, T.R.; Mills, G.; Christen, A.; Voogt, J.A. *Urban Climates*; Cambridge University Press: Cambridge, UK, 2017.
8. Apritasari, Y.D.; Indraprastha, A.; Wonorahardjo, S. The Role of Building Mass Configuration and Material Selection for Mitigating the Intensity of the Urban Heat Island. *Energy Build.* **2024**, *323*, 114822. [CrossRef]
9. Aghamolaei, R.; Fallahpour, M.; Mirzaei, P.A. Tempo-Spatial Thermal Comfort Analysis of Urban Heat Island with Coupling of CFD and Building Energy Simulation. *Energy Build.* **2021**, *251*, 111317. [CrossRef]

10. Mohamed, A.A.; Odindi, J.; Mutanga, O. Land Surface Temperature and Emissivity Estimation for Urban Heat Island Assessment Using Medium- and Low-Resolution Space-Borne Sensors: A Review. *Geocarto Int.* **2017**, *32*, 455–470. [CrossRef]
11. Preet, S.; Mathur, S.; Mathur, J.; Sharma, M.K.; Chowdhury, A. Energy Characterization of Forced Ventilated Photovoltaic-DSF System in Hot Summer of Composite Climate. *Energy Built Environ.* **2024**, *5*, 704–718. [CrossRef]
12. Santamouris, M. On the Energy Impact of Urban Heat Island and Global Warming on Buildings. *Energy Build.* **2014**, *82*, 100–113. [CrossRef]
13. Bostancioglu, E. Double Skin Façade Assessment by Fuzzy AHP and Comparison with AHP. *Archit. Eng. Des. Manag.* **2021**, *17*, 110–130. [CrossRef]
14. Wang, Y.; He, F.; Lv, Z.; Yang, W.; Wang, Q. Experimental Investigations on Thermal Performance of Spray Cooling Double Skin Façade in Hot Humid Climate Region. *Energy Build.* **2022**, *277*, 112605. [CrossRef]
15. Karunyasopon, P.; Park, D.Y.; Le, D.M.; Chang, S. Performance Analysis of Transparent BIPV/T Double Skin Façades Integrated with the Decision-Making Algorithm for Mixed-Mode Building Ventilation. Archit. *Eng. Des. Manag.* **2023**, *20*, 1141–1163. [CrossRef]
16. Souza, C.O.L.; Souza, H.A.; Rodrigues, E.F. Experimental and Numerical Analysis of a Naturally Ventilated Double-Skin Façade. *Energy Build.* **2018**, *165*, 328–339. [CrossRef]
17. Halawa, E.; Ghaffarianhoseini, A.; Ghaffarianhoseini, A.; Trombley, J.; Hassan, N.; Baig, M.; Yusoff, S.Y.; Ismail, M.A. A Review on Energy Conscious Designs of Building Façades in Hot and Humid Climates: Lessons for (and from) Kuala Lumpur and Darwin. Renew. *Sustain. Energy Rev.* **2018**, *82*, 2147–2161. [CrossRef]
18. Sadatiseyedmahalleh, S.; Li, X. Fast Assessment Method of Annual Energy Consumption for DSF and SSFs. *Build. Environ.* **2024**, *251*, 111164. [CrossRef]
19. Gennaro, G.; Catto Lucchino, E.; Goia, F.; Favoino, F. Modelling Double Skin Façades (DSFs) in Whole-Building Energy Simulation Tools: Validation and Inter-Software Comparison of Naturally Ventilated Single-Story DSFs. *Build. Environ.* **2023**, *231*, 110002. [CrossRef]
20. An, Y.; Choi, H.; Kim, E.; Kim, T. Experimental Analysis of Seasonal Temperature Characteristics and Cooling and Heating Energy Consumption of a Slim Double-Skin Window. *Energy Build.* **2022**, *256*, 111681. [CrossRef]
21. Yoon, N.; Heo, Y. Weather-Based Operation Strategy for a Dynamically Compartmentalized Double-Skin Façade System. *Build. Environ.* **2022**, *226*, 109755. [CrossRef]
22. Sanchez, E.; Rolando, A.; Sant, R.; Ayuso, L. Influence of Natural Ventilation Due to Buoyancy and Heat Transfer in the Energy Efficiency of a Double Skin Façade Building. *Energy Sustain. Dev.* **2016**, *33*, 139–148. [CrossRef]
23. Lou, W.; Huang, M.; Zhang, M.; Lin, N. Experimental and Zonal Modeling for Wind Pressures on Double-Skin Facades of a Tall Building. *Energy Build.* **2012**, *54*, 179–191. [CrossRef]
24. Saroglou, T.; Theodosiou, T.; Givoni, B.; Meir, I.A. Studies on the Optimum Double-Skin Curtain Wall Design for High-Rise Buildings in the Mediterranean Climate. *Energy Build.* **2020**, *208*, 109641. [CrossRef]
25. Sharston, R.; Singh, M. The Role of Passive, Active, and Operational Parameters in the Relationship between Urban Heat Island Effect (UHI) and Building Energy Consumption. *Energy Build.* **2024**, *323*, 114720. [CrossRef]
26. Pelletier, K.; Wood, C.; Calautit, J.; Wu, Y. The Viability of Double-Skin Façade Systems in the 21st Century: A Systematic Review and Meta-Analysis of the Nexus of Factors Affecting Ventilation and Thermal Performance, and Building Integration. *Build. Environ.* **2023**, *228*, 109870. [CrossRef]
27. Jankovic, A.; Gennaro, G.; Chaudhary, G.; Goia, F.; Favoino, F. Tracer Gas Techniques for Airflow Characterization in Double Skin Facades. *Build. Environ.* **2022**, *212*, 108803. [CrossRef]
28. Darkwa, J.; Li, Y.; Chow, D.H.C. Heat Transfer and Air Movement Behaviour in a Double-Skin Façade. *Sustain. Cities Soc.* **2014**, *10*, 130–139. [CrossRef]
29. Mansouri, S.T.; Zarghami, E. Investigating the Effect of the Physical Layout of the Architecture of High-Rise Buildings, Residential Complexes, and Urban Heat Islands. *Energy Built Environ.* **2025**, *6*, 1–17. [CrossRef]
30. Central Weather Administration, Ministry of Transportation and Communications. CODiS. 2024. Available online: https://codis.cwa.gov.tw/ (accessed on 1 August 2023).
31. Kim, D.D. Computational Fluid Dynamics Assessment for the Thermal Performance of Double-Skin Façades in Office Buildings under Hot Climatic Condition. *Build. Serv. Eng. Res. Technol.* **2020**, *42*, 45–61. [CrossRef]
32. Alberto, A.; Ramos, N.M.M.; Almeida, R.M.S.F. Parametric Study of Double-Skin Facades Performance in Mild Climate Countries. *J. Build. Eng.* **2017**, *12*, 87–98. [CrossRef]
33. Franke, J.; Hellsten, A.; Schlünzen, H.; Carissimo, B. Best Practice Guideline for the CFD Simulation of Flows in the Urban Environment, Technical Report, COST European Cooperation in Science and Technology. 2007. Available online: https://hal.science/hal-04181390 (accessed on 1 December 2023).
34. Ding, W.; Hasemi, Y.; Yamada, T. Natural Ventilation Performance of a Double-Skin Façade with a Solar Chimney. *Energy Build.* **2005**, *37*, 411–418. [CrossRef]

35. Tao, Y.; Zhang, H.; Zhang, L.; Zhang, G.; Tu, J.; Shi, L. Ventilation Performance of a Naturally Ventilated Double-Skin Façade in Buildings. *Renew. Energy* **2021**, *167*, 184–198. [CrossRef]
36. Oberkampf, W.L.; Trucano, T.G.; Hirsch, C. Verification, Validation, and Predictive Capability in Computational Engineering and Physics. *Appl. Mech. Rev.* **2004**, *57*, 345–384. [CrossRef]
37. Sih-Huan, W.; Chih-Hong, H. The Vertical Enthalpy Distribution of Canopy Heat Islands in Metropolitan Area. In Proceedings of the 16th Academic Symposium on Technology and Society 2020, Chung Hua University, Hsinchu, Taiwan, 6 June 2020.

Disclaimer/Publisher's Note: The statements, opinions and data contained in all publications are solely those of the individual author(s) and contributor(s) and not of MDPI and/or the editor(s). MDPI and/or the editor(s) disclaim responsibility for any injury to people or property resulting from any ideas, methods, instructions or products referred to in the content.